

Portable Ultrasound Data Acquisition System Design

Dusa Chandrashekar

A Dissertation Submitted to
Indian Institute of Technology Hyderabad
In Partial Fulfillment of the Requirements for
The Degree of Master of Technology



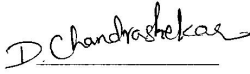
भारतीय प्रौद्योगिकी संस्थान हैदराबाद
Indian Institute of Technology Hyderabad

Department of Electrical Engineering

July 2015

Declaration

I declare that this written submission represents my ideas in my own words, and where ideas or words of others have been included, I have adequately cited and referenced the original sources. I also declare that I have adhered to all principles of academic honesty and integrity and have not misrepresented or fabricated or falsified any idea/data/fact/source in my submission. I understand that any violation of the above will be a cause for disciplinary action by the Institute and can also evoke penal action from the sources that have thus not been properly cited, or from whom proper permission has not been taken when needed.



(Signature)

Dusa Chandrashekar

EE12M1014

(Roll No.)

Approval Sheet

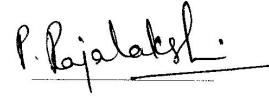
This Thesis entitled Portable Ultrasound Data Acquisition System Design by Dusa Chandrashekar is approved for the degree of Master of Technology from IIT Hyderabad



(Dr. Ch. Sobhan Babu) Examiner
Dept. Computer Science and Engineering
IITH



(Dr. Sumohana Channappayya) Examiner
Dept. of Electrical Engineering
IITH



(Dr. P. Rajalakshmi) Adviser
Dept. of Electrical Engineering
IITH

Acknowledgements

The work presented here would not have been possible without the guidance and support of people who in one way or other extended their valuable assistance. I take this opportunity to express my sincere gratitude towards them. First and foremost, I would like to thank my supervisor Dr. P. Rajalakshmi for her phenomenal valuable guidance and support. I am also grateful to our ultrasound team for great team efforts.

Abstract

Ultrasound is radiation-free, patient-friendly and less expensive when compared to other medical imaging techniques. Ultrasound scanning have the capability to image the organs in real time, thus offering quick diagnosis. Conventional medical ultrasound machines are not suited for remote health monitoring because of their large form factor and lack of trained sonographers limiting its use only to urban areas and well trained clinicians. This thesis discusses the implementation of portable ultrasound data acquisition system for Point of Care (POC) applications in both of the system-level Hardware and Firmware design level. In the Hardware design, we are targeting the compactable application as well as the extendable applications where the power, level of integration and the feasible of the replication are critical. The portable system architecture for 8-channel consists of ASICs for ultrasound and FPGA. Beamforming is the front end process to steer and focus the acoustic beam with in the region of interest for diagnosis. The main components that have the greatest influence on the hardware design and system performance of the signal-processing board are the Analog Front End (AFE), logic pulse driver, High Voltage pulser and FPGA. Typically analog beamformers uses bulky lumped L-C delay lines and complex switching circuitry. The digital beamformers can implement the digital circuitry for dynamic focusing with reduced size and cost. We could utilize the TI AFE5808 as the analog front end of the data acquisition by using its eight ADC in one IC as well as using the LM96570 the ultrasound transmitter as an integrated solution for sending a full control ultrasound signal over selecting beam directions for eight channels. This lead to a significant decrease of the size, cost and the power making from the proposed design an ideal solution for the low-cost ultrasound imaging devices. The proposed design is validated by scanning the customized phantom and acquired the ultrasound image. The prototype of our data acquisition system is also validated with NI's PXIe-1078 and Biosono front end platforms , reconstructed the ultrasound image by scanning the phantom.

Contents

Declaration	ii
Approval Sheet	iii
Acknowledgements	iv
Abstract	v
1 Thesis Overview	1
1.1 Thesis Overview and Problem Definition	1
1.2 Basics of Ultrasound Physics	2
1.2.1 Tx Acoustic focusing and Steering	2
1.2.2 Receive focusing	3
1.3 Basic Principle of Ultrasound Imaging	4
1.3.1 Modes of Ultrasound Imaging	5
1.4 Thesis Objective and Contribution	7
2 Hardware architecture for Ultrasound Data Acquisition System (Ultrasound DAQ)	8
2.1 Introduction	8
2.2 System Architecture	9
2.2.1 Transducer array	9
2.2.2 Logic Pulse Driver	11
2.2.3 HV pulser	12
2.2.4 Analog Front End (AFE)	13
2.2.5 User interface	14
2.2.6 Main features of the proposed ultrasound transmit platform	15
2.2.7 Comparative study with literature	15
2.3 Conclusion	16
3 Digital Ultrasound beamformer	17
3.1 Introduction	17
3.2 Transmit Beamforming Architecture	18
3.3 Receive Beamforming Architecture	20
3.4 ASIC Implementation	22
3.5 Conclusion	22

4	Validation and Evaluation of the prototype	24
4.1	Introduction	24
4.2	Prototype of secured, IoT enabled portable ultrasound system	24
4.2.1	Phantom Experiment with Our Portable Ultrasound Imaging System	25
4.3	Validation With other Platforms	25
4.3.1	PXI System	25
4.3.2	Biosono Frontend Platform	26
4.4	Calculations for B-Mode Imaging	27
5	Conclusions	30
5.1	Review of Thesis Work	30
5.2	Conclusions	30
	References	32

List of Figures

1.1	Focusing of Ultrasound energy.	3
1.2	Delays to excite ultrasound elements to steer the acoustic beam.	3
1.3	Receive focusing with no delays.	4
1.4	Receive focusing with no delays for coherent sum.	4
1.5	Block diagram of basic ultrasound imaging system architecture	5
1.6	Pulse Repetition Frequency calculation	6
1.7	Steering and Focusing of the acoustic beam.	6
2.1	Block diagram of ultrasound imaging system architecture	9
2.2	programmable 8-channel Ultrasound Data Acquisition System	9
2.3	Different types of transducers.	10
2.4	Linear and phased array excitation.	10
2.5	Principle of phased array transducer	11
2.6	4-wire serial interface timing diagrams.	11
2.7	Block diagram of the logic pulse driver with Pattern and Delay Generator.	12
2.8	Logic pulses of two channels	12
2.9	Orcad schematic for Logic pulse driver board.	13
2.10	Table for HV out voltage level W.r.t differential logic inputs.	13
2.11	HV pulses with P and N logics	14
2.12	Orcad schematic for HV pulser board.	14
2.13	Functional block diagram of Analog Frontend.	15
2.14	User interface to control the transmission parameters	15
2.15	LabVIEW project interfaced to Spartan-3E FPGA Starter Kit	16
3.1	The ultrasound imaging system architecture with the proposed digital beamformer	18
3.2	Calculations of delay profile for a steering angle (α°)	19
3.3	Modular architecture for proposed Transmit beamforming	20
3.4	Simulation results	20
3.5	Modular architecture for proposed receive beamforming.	21
3.6	Simulation result of Rx beamforming design.	21
3.7	Gate level simulation results in Design Compiler.	22
3.8	Layout of ASIC of proposed architecture for integrated Tx and Rx beamformer.	23
4.1	Prototype of secure and IoT enabled potable ultrasound systems	25
4.2	Portable ultrasound scanner module.	25

4.3	Acquired ultrasound image from phantom.	27
4.4	Validation with PXI platform.	27
4.5	Acquired ultrasound image with PXI setup.	28
4.6	Biosono Platform.	28
4.7	Acquired ultrasound image using Biosono frontend board.	29
4.8	Spatial Resolution of ultrasound image.	29

Chapter 1

Thesis Overview

1.1 Thesis Overview and Problem Definition

Ultrasound imaging is the safest and easiest diagnostic technique for real time imaging of patient organs. Ultrasound imaging is regularly used in cardiology, obstetrics, gynaecology, abdominal imaging, etc. Its popularity arises from the fact that it provides high-resolution images without the use of ionizing radiation [1]. It is also mostly non-invasive, although an invasive technique like intra-vascular imaging is also possible. Medical ultrasound has gained popularity in the clinical practice as a quick, compact, and affordable diagnostic tool. It has the advantage over computed tomography and magnetic resonance imaging methods in that the preparation for a scan is minimal, and no health hazards are involved.

The commercially available machines are not useful for research purposes, in most of the cases their architecture is closed for the researcher [2]. The POC applications requires a portable medical devices to offer quick diagnosis. But the commercially available machines are limited well-established hospitals, urban areas and diagnostic centres, due to their form factor [3]. Basically beamforming is the front processing of the ultrasound, before it was based on the analog processing and it had the disadvantage of the analog world. On the other hand by utilizing the digitalization of the modern digital beamformer and making it signal processing based technique used in sensor arrays for directional signal transmission or reception [4]. This is achieved by combining elements in the array in such a way that signals at particular angle experience constructive interference and while others experience destructive interference. Beamforming can be used at both the transmitter and receiver side to achieve spatial selectivity. Beamforming can be used for both radio and sound waves. It has found numerous applications in radar; sonar, seismology, wireless communications, radio astronomy, speech, acoustics, and biomedicine.

1.2 Basics of Ultrasound Physics

Acoustic waves are mechanical waves i.e. acoustic energy is transferred between two points in the medium while leaving the intervening medium essentially unchanged after transfer. The piezoelectric sensors are used to generate the ultrasound. The pressure applied to the sensor is proportional to voltage developed across it. In the same way an oscillating voltage applied to the sensor makes it to generate the mechanical vibration. The speed with which the acoustic wave can travel is determined by the properties of the medium. The properties of primary influence to the waves are the density and bulk modulus. The speed of the sound is given by

$$c = \sqrt{k\rho}$$

Where ρ is material density (in Kg/m³), and k is the adiabatic bulk modulus.

The Characteristic acoustic impedance, like its electrical counterpart, is a measure of the opposition of the medium to the propagation of a sound wave. When two mediums have a similar acoustic impedance they can be said to be matched and sound waves will transfer between them with very little reflection. For normal incident waves, this impedance measure behaves similarly to its electrical counterpart, and reflection (R) and transmission (T) coefficients for waves travelling from material 1 to material 2 can be calculated as the following equations

$$R = \left(\frac{Z_1 - Z_2}{Z_1 + Z_2} \right)^2$$

$$T = \frac{4 + Z_2 + Z_1}{(Z_2 + Z_1)^2}$$

where as Z_1 and Z_2 are acoustic impedances of medium 1 and 2 respectively.

1.2.1 Tx Acoustic focusing and Steering

A plane wave will tend to spread from the edges as it travels using a process of diffraction. This phenomenon is described by the Huygens-Fresnel principle, which describes each point on a wave front as a source for an expanding radial wave. As the wave expands, its energy is spread across a greater region. The further the wave has travelled, the greater the reduction in wave amplitude, and the greater the reduction in amplitude of any reflections from the wave. In order to create a high amplitude wave-front (to improve the echo strength) the energy from the wave can be focused. Focusing the wave controls the travel path of the acoustic energy so that its signal strength is maximized within a desired region as shown Fig. 1.1.

In order to be able to control the focus, a new type of transducer needs to be considered, and a new way of exciting it. An array transducer divides the transducer surface into sub regions, each of which can be controlled separately through separate electrical connections. The subdivided regions of an array are referred to as elements. When each element in an array is excited at different times, the diffraction of the individual wave fronts generated from each element can be planned in order to create a focused pulse as shown in Fig. 1.2.

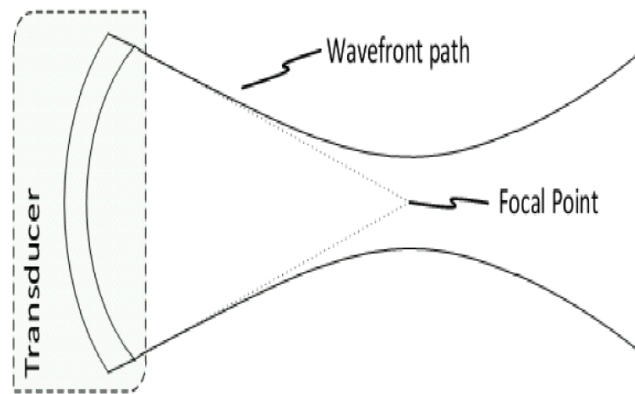


Figure 1.1: Focusing of Ultrasound energy.

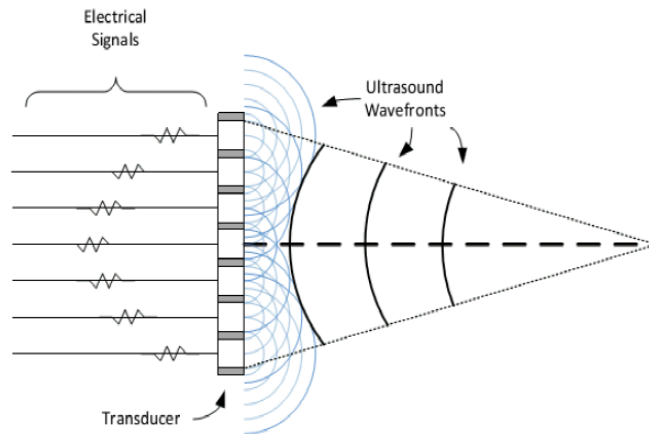


Figure 1.2: Delays to excite ultrasound elements to steer the acoustic beam.

1.2.2 Receive focusing

An electrical pulse applied to a transducer will generate a sound wave and vice versa. This is how the echoes generated in the medium and propagated further the reflected signals are received. After a sound pulse is transmitted, the transducer begins to listen for reflections. When the reflections arrive back at the transducer they are converted into electrical signals, and the amplitude of the signals is proportional to the pressure of the sound wave that created them. In this case, the fundamental frequency of the transducer acts as a carrier signal, with its amplitude indicating the reflection size. The echo signal is extracted by taking the envelope of the received signal. In a geometrically focused transducer, signals from the focal region will arrive at the same time at the transducer surface, and thus create a large electrical signal. In an array, however, the signals will all arrive at different times at each element.

The Fig. 1.3 and Fig. 1.4 are shows the receive focusing without and with delays respectively. The differences in signal arrival time at each element need to be compensated for by delaying the electrical signals after they are received. If the same transmit delays are applied to the received

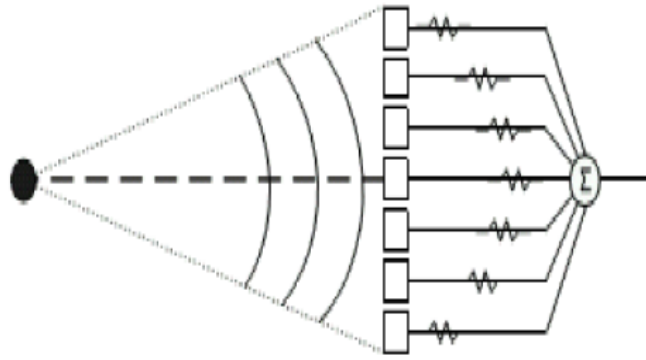


Figure 1.3: Receive focusing with no delays.

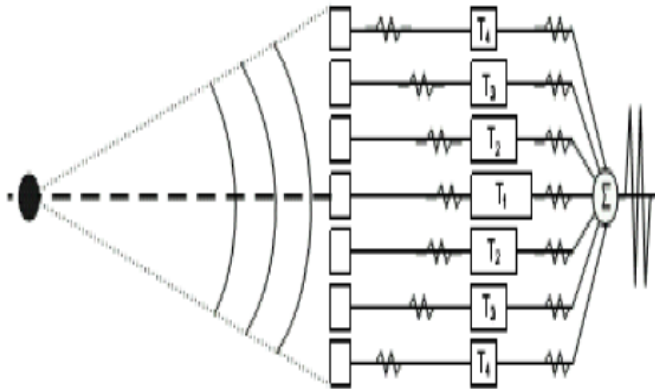


Figure 1.4: Receive focusing with no delays for coherent sum.

signals, then waves originating from the focal region will constructively interfere, increasing their amplitude. Signals from outside of this region will not be aligned, and will tend to destructively interfere, reducing their impact on the final output. This process will create the same amplitude of signal as occurs due to a geometric focus. The process of delaying the received signals in order to create focus is called beamforming. Beamforming is the inverse operation of transmit focusing, so all of the details discussed previously applying to transmit focusing, also apply to receive focusing.

1.3 Basic Principle of Ultrasound Imaging

The basic functional block diagram for ultrasound imaging system is shown in Fig. 1.5. The term ultrasound refers to frequencies that are greater than 20 kHz, which is commonly accepted to be the upper frequency limit the human ear can hear. Typically, ultrasound systems operate in the 2 MHz to 20 MHz frequency range, although some systems are approaching 40 MHz for harmonic imaging. The basic principle of ultrasound system is to focus sound waves along a given scanline so that the waves constructively add together at the desired focal point. As the sound waves propagate

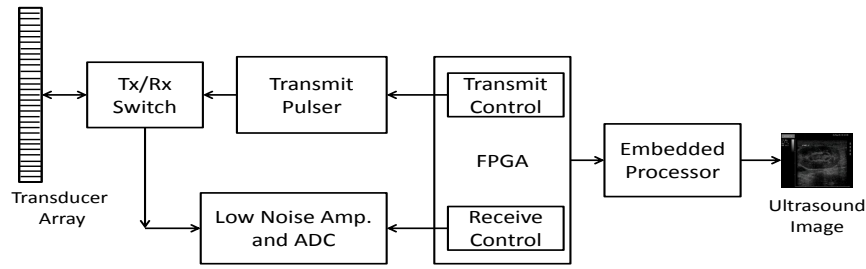


Figure 1.5: Block diagram of basic ultrasound imaging system architecture

towards the focal point, they reflect off on any object they encounter along their propagation path. The reflected waves have been acquired with the transducers, next transmission follows towards a new focal point along a scanline. After the sound waves along the given scanline acquired, the ultrasound system focuses along a new scan line until all of the scan lines in the desired region of interest have been measured. To focus the sound waves towards a particular focal point, a set of transducer elements are energized with a set of time-delayed pulses to produce a set of sound waves that propagate through the region of interest, which is typically the target organ and the surrounding tissue. This process of using multiple sound waves to steer and focus a beam of sound is commonly referred to as beamforming [5].

Once the transducers have generated their respective sound waves, they become sensors that detect any reflected sound waves that are created when the transmitted sound waves encounter a change in tissue density within the region of interest. By properly time delaying the pulses to each active transducer, the resulting time-delayed sound waves meet at the desired focal point that resides at a pre-computed depth along a known scan line. The amplitude of the reflected sound waves forms the basis for the ultrasound image at this focal point location. Envelope detection is used to detect the peaks in the received signal and then log compression is used to reduce the dynamic range of the received signals for efficient display. Once all of the amplitudes for all of the focal points have been detected, they can be displayed for analysis by the doctor or technician. Since the coordinate system, in which the ultrasound system usually operates, does not match the display coordinate systems, a coordinate transformation, called scan conversion, needs to be performed before being displayed on a CRT monitor.

1.3.1 Modes of Ultrasound Imaging

The ultrasound systems are operated in following modes for ultrasound imaging.

- A Mode: Amplitude of echoes determines intensity of pixel.
- CW Mode: To image moving targets with fixed position of transducer.

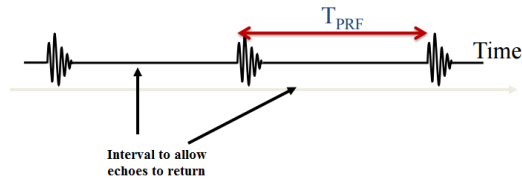


Figure 1.6: Pulse Repetition Frequency calculation

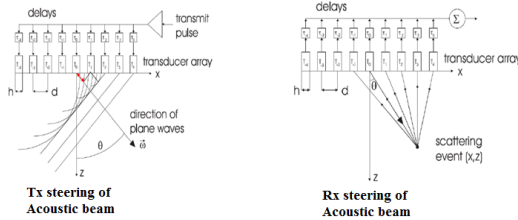


Figure 1.7: Steering and Focusing of the acoustic beam.

- B Mode: Tx and Rx steering and focusing of ultrasound beam.
- C Mode: Colour Doppler - Shift in frequency is used for detecting Blood Flow.

A-mode of Imaging

- It is pulse-echo imaging.
- Sequentially array of sensors are excited and acquires scanlines of the image.
- Transmit frequency depends on application of diagnosis.
- High transmit frequencies for superficial organ imaging.
- The depth of the target determines the transducer receive time. i.e. $t = \frac{2*d}{c}$, where $c = 1540m/s$
- Fig. 1.6 show the calculation of PRF for pulse echo imaging.

B-mode of Imaging

- Here the acoustic beam is steered in the transducer field of view.
- Applying transmit delays patterns in excitation creates constructive interference at focal point.
- The number of focal points are limited by standard frame rate.
- While in receiving mode, the echo signals are summed coherently to form image scanlines.
- The scanlines are stacked to form the ultrasound image.
- Fig. 1.7 show the calculation of PRF for pulse echo imaging.

1.4 Thesis Objective and Contribution

The goal of the thesis has been the development of a ultrasound data acquisition system in both Hardware and Firmware level. The hardware design includes high performance ultrasound ASICs. The digital Tx and Rx ASICs make the hardware extremely portable. In commercially available systems are large in size because of following reasons,

- Bulky analog L-C delay lines are used for beamforming.
- High voltage MOSFET circuits are used to amplify the logic pulses.

So, we have implemented the hardware with ultrasound ASICs. Typically the ultrasound systems are big due to the hardware provided for data acquisition. These Tx and Rx ASICs reduced the size of the hardware of data. The digital beamformer instead of analog architecture, which provides accurate control of the acoustic beam steering and focusing in the region of interest.

Our contribution in the hardware design is to design and implemented the portable and compact architecture. We could utilize the TI LM96570, MAX14808, and AFE5808 to transmit and receive the ultrasound in to patient tissue. Here the MAX14808 is to amplify the logic pulses and also work as Tx/Rx switch which can protect the AFE from the high voltage excitation pulses. Where as the Firmware is to control the hardware to generate a sharp and focused at different focal points. The digital beamforming as firmware is implemented on FPGA.

Chapter 2

Hardware architecture for Ultrasound Data Acquisition System (Ultrasound DAQ)

2.1 Introduction

The adoption of this modality by all categories of hospitals and other health care institutions has given rise to new designs and market opportunities [6]. In modern ultrasound imaging systems, the ultrasound transmit module consists of digital Transmit (Tx) beamformer typically generates necessary logic pulses with proper timing and phase to enable electronic steer and focus of the acoustic beam. However, these systems often "closed" architecture provides the researchers to have limited access to the ultrasound transmit module [7].

Recently, Amauri et al. in [8] discussed the development of programmable FPGA based 8 independent channel Arbitrary Waveform Generator (AWG) for medical ultrasound research activities. However, this AWG transmit platform requires additional expensive electronics includes high voltage MOSFET drivers, Transformers. The digital Tx beamformer is configured using FPGA device for accurate control on transmission parameters such as center frequency and pulse pattern length to optimize image quality based on the medical application. FPGAs improve the ability for ultrasound imaging systems to create small form factor and high-performance products with reduced power consumption [9]. In [10], Gabriella et. al. have proposed a new beamforming technique in which the transmit aperture apodization by varying the length of the excitation pulses.

This chapter presents the hardware architecture of a programmable FPGA based 8-channel ultrasound data acquisition system for medical ultrasound researches. Our design uses FPGA to configure the logic pulse driver with single high speed 4-wire serial interface for transmission parameters such as delay profile for acoustic beam steering, transmit frequency, and pulse length depending on medical application. Pre-calculated delay profile is updated to pulse driver per each transmission in different steering angles. We have conducted an experiment by transmitting ultrasound into gelatin phantom. The electrical signals of echoes from each focal point are acquired by AFE module and further applied to signal processing algorithms for ultrasound imaging.

2.2 System Architecture

Fig. 3.1 shows the block diagram for ultrasound imaging system architecture. The architecture mainly consists of transducer array, High Voltage (HV) pulser, digital logic pulse driver, FPGA device, Analog Front End (AFE) and signal processing modules. The basic principle for an ultrasound imaging system is to transmit ultrasound burst signal into the area of interest of organ, receive echoes and process for imaging [11]. The proposed design of ultrasound transmitter reflects the same principle with user interface to enable flexibility in modifying the transmission parameters. Here digital pulse driver is configured using SPI controlling signals from FPGA. With FPGA device, we programmed the internal registers of digital pulse driver to change delay profile for each channel, frequency of diagnosis and pulse length depending on the medical application. The Fig. 2.2 shows the complete hardware for data acquisition system.

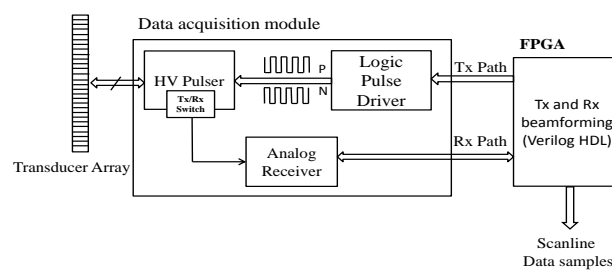


Figure 2.1: Block diagram of ultrasound imaging system architecture

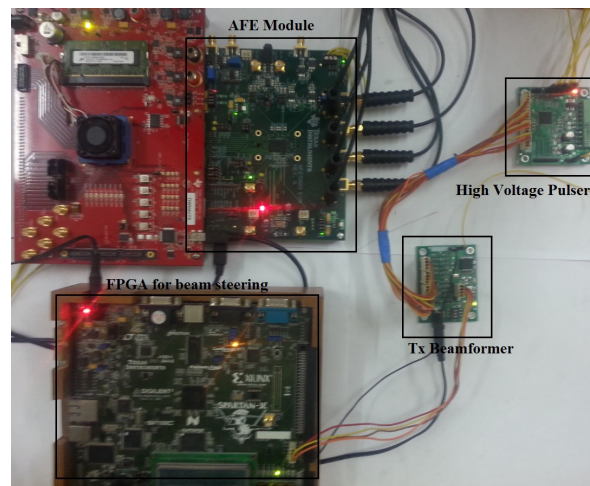


Figure 2.2: programmable 8-channel Ultrasound Data Acquisition System

2.2.1 Transducer array

Typically the transducer arrays are four types, they are

- Linear sequential array

- Linear phased array
- Curvilinear sequential array
- Curvilinear phased array

Here the linear and phased indicates the shape of the probe head, in linear type the elements are placed in sequential array where as in curvilinear array the elements are placed in convex shape. The transducers of different types are show in Fig. 2.3. The transducer elements of linear and curvilinear sequential arrays are excited in sequentially one after the other. Every transmission and receive can form one scanline of the ultrasound image. Typically the sequential arrays are provided to have large active aperture which can cover large field of view. The phased array elements are excited in particular delay patterns to steer and focus the acoustic beam. Each transmission of steer and focus in a given angle of direction can form a scanline of the image.

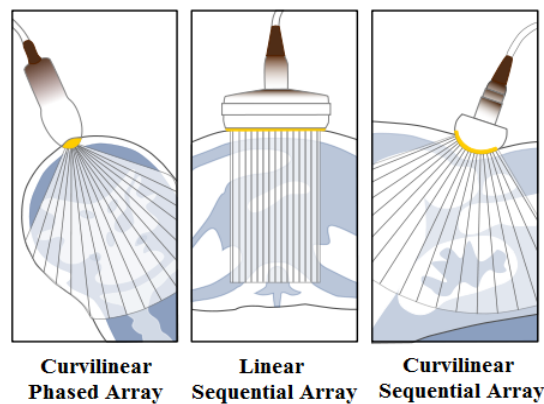


Figure 2.3: Different types of transducers.

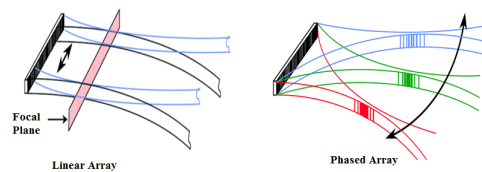


Figure 2.4: Linear and phased array excitation.

The medical ultrasound imaging transducers are excited in two modes: linear and phased array mode. In linear array mode, subset of transducer elements are excited where as in phased array mode all the elements of transducer are excited to focus the sharp ultrasound beam at focal point as shown in Fig. 2.4. For a transducer array, the piezoelectric element pitch size is required to be smaller than half of the wavelength [12]. To scan interest of organ, the ultrasound beam should be focused at multiple focal points. The time delays are applied to excitation of sensor elements to create constructive interference of wave fronts at different focal points. The number focal points are limited by the standard frame rates. Because more the number of focal points more time it takes to acquire one frame. The basic principle of phased array transducer excitation is shown in Fig. 2.5.

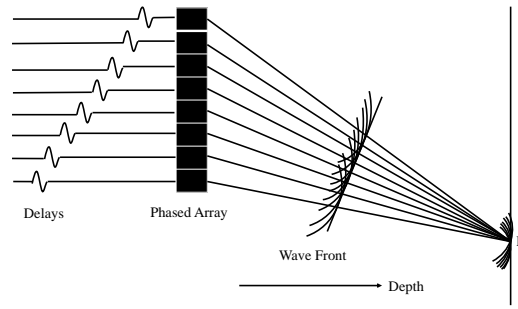


Figure 2.5: Principle of phased array transducer

2.2.2 Logic Pulse Driver

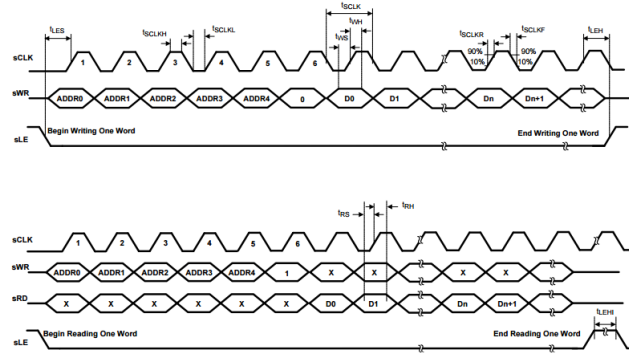


Figure 2.6: 4-wire serial interface timing diagrams.

The proposed design uses a 8-channel programmable logic pulse driver (LM96570) to generate proper phased logic pulses by programming with FPGA. The 4-wire serial interface programming timings are shown in Fig. 2.6. Fig. 2.7 shows the block diagram of the logic pulse driver to generate pulse patterns and delay pattern generator. The pulse driver has internal programmable registers, which can be programmed to configure transmission parameters at a maximum data rate of 80Mbps [13].

Overall 27 programmable registers to programme transmission parameters. Address 00-07h registers of each 22 bit for delay pattern, in which LSB 3-bits for fine delay and next 9-bits are coarse delay. Where as the address 08-17h registers are for pulse pattern. A control register (1Ah) is used to change frequency of diagnosis and pulse length for medical diagnosis better resolution can be achieved at higher frequency, on other side with lower the frequency depth of view will be increased. It is configured to generate short ultrasound pulses to improve lateral resolution. The Tx beam-forming technique is to generate time delayed logic inputs to focus ultrasound beam at focal point, this improves resolution of image. The level of improvement in resolution of ultrasound image depends on minimum time delay of Tx beamformer. The phased logic pulses of two different channels with 64 pulse pattern length are shown in Fig. 2.8. Each of the 8 output channels are designed to

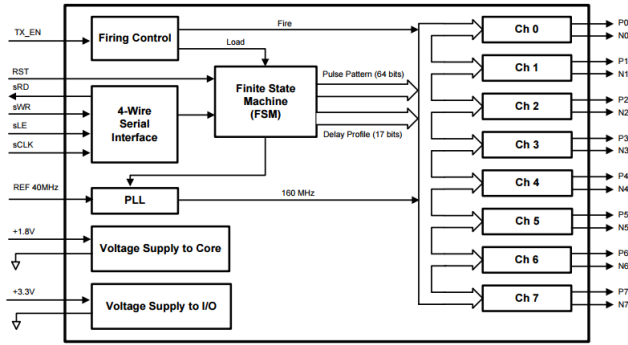


Figure 2.7: Block diagram of the logic pulse driver with Pattern and Delay Generator.

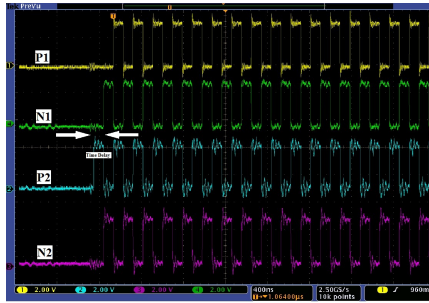


Figure 2.8: Logic pulses of two channels

drive the positive and negative pulse control CMOS 3.3v logic inputs, P_n and N_n , respectively, of a high-voltage ultrasound pulser. With reference to the data sheet, the schematic for the logic pulse driver board is design with LM96570 and discrete components. The Fig. 2.9 shows Orcad Schematic designed for logic pulse driver.

2.2.3 HV pulser

Most of the ultrasound imaging systems uses MOSFET drivers to generate high voltage pulses to excite ultrasound sensors, Cathode Ray Tube(CRT) for displaying ultrasound image and transducer interfacing circuits makes the system size bulky. For ultrasound applications the frequency of operation is 2-20Mhz, so HV pulser device generates high-frequency, high voltage bipolar pulses from low-voltage control logic inputs to drive piezoelectric sensors. The HV pulser simply acts as Digital to Analog Converter (DAC) to amplify the digital outputs of beamformer. Typically the ultrasound sensors are excited at high voltage (100 Vpp) and high frequencies (2-20 Mhz) [14]. The HV pulser used in the proposed architecture can also acts as switch to receive ultrasound reflected signal from tissue. Two logic inputs to pulser control functionality as Rx switch and as DAC amplifier. The HV pulser used in the proposed architecture can also acts as switch to receive ultrasound reflected signal from tissue.

The output of the HV pulser is controlled by two differential logic pulses from pulse driver (Fig. 2.10). If two inputs are logic one then the pulser circuit can act as receive switch to receive low voltage signals of reflected ultrasound waves and prevent overloading of AFE module. If two inputs are logic zero then output of pulser is zero. When two inputs are different logic then it generates

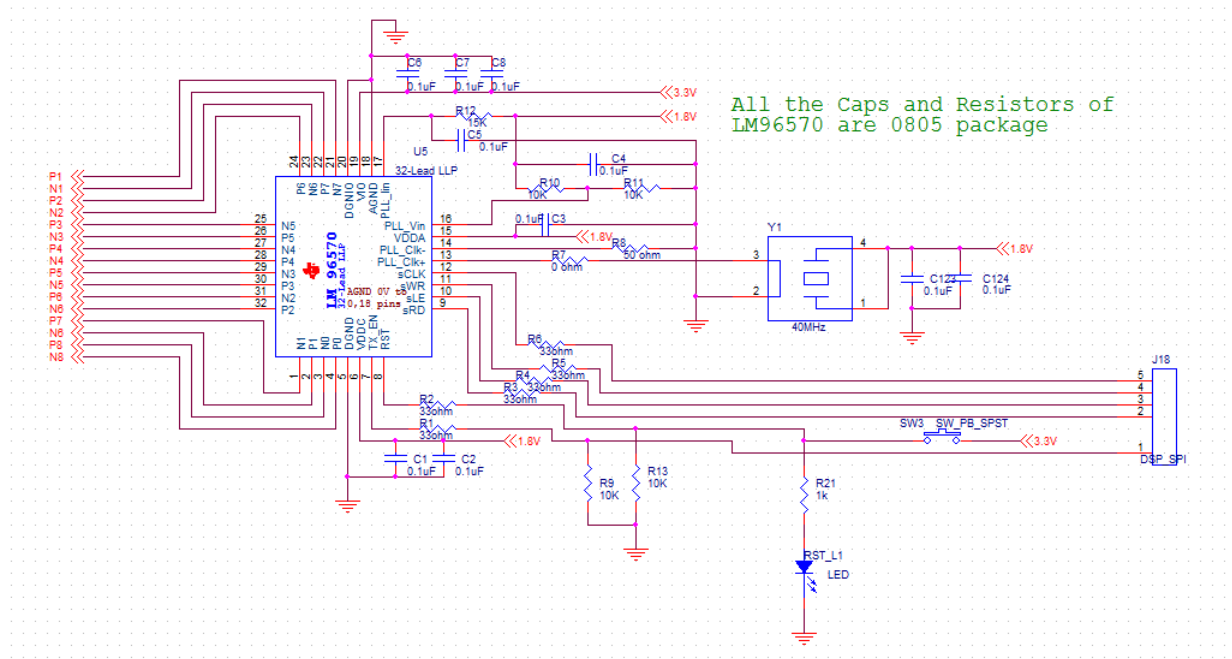


Figure 2.9: Orcad schematic for Logic pulse driver board.

bipolar high voltages. Fig. 2.11 shows P and N logic pulses from the beamformer and corresponding high voltage signal. With reference to the data sheet, the schematic for the logic pulse driver board is design with MAX14808 and desrete components as shown in Fig. 2.12.

INPUTS		OUTPUTS	
DINN_	DINP_	OUT_	LVOUT_ (MAX14808 ONLY)
0	0	High impedance (damp off)	T/R switch off (LVOUT_ = GND)
1	0	High impedance (damp off)	T/R switch off (LVOUT_ = GND)
0	1	High impedance (damp off)	T/R switch off (LVOUT_ = GND)
1	1	High impedance (damp on)	T/R switch on

0 = logic-low, 1 = logic-high

Figure 2.10: Table for HV out voltage level W.r.t differential logic inputs.

2.2.4 Analog Front End (AFE)

Typical ultrasound AFE module includes Low Noise Amplifier (LNA), Time-Gain-Compensation (TGC) amplifier, Continuous Wave (CW) mixer and A/D converter (ADC) [15]. In our design high performance AFE is used to acquire low voltage signals, time gain compensation, filtering, and digitizing, where the outputs samples are in Low Voltage Differential Signal (LVDS) format. The LVDS outputs are further de-serialized in FPGA. Fig. 2.13 shows the functional block diagram of Analog front end ASIC. The ASIC is an integrated 8 ADCs whose output is in LVDs format. Voltage controlled attenuator to implement Time gain compensation for reflected signals. This is provided with SPI interface to programme the received signal conditioning parameters. The ADC sampling frequency is 40 MHz or 65 MHz can be programmed through SPI interface.

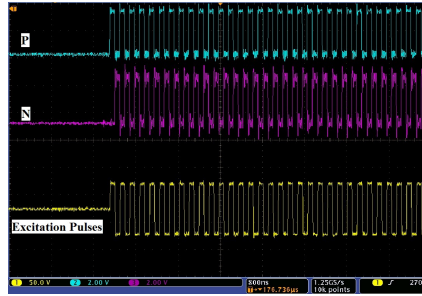


Figure 2.11: HV pulses with P and N logics

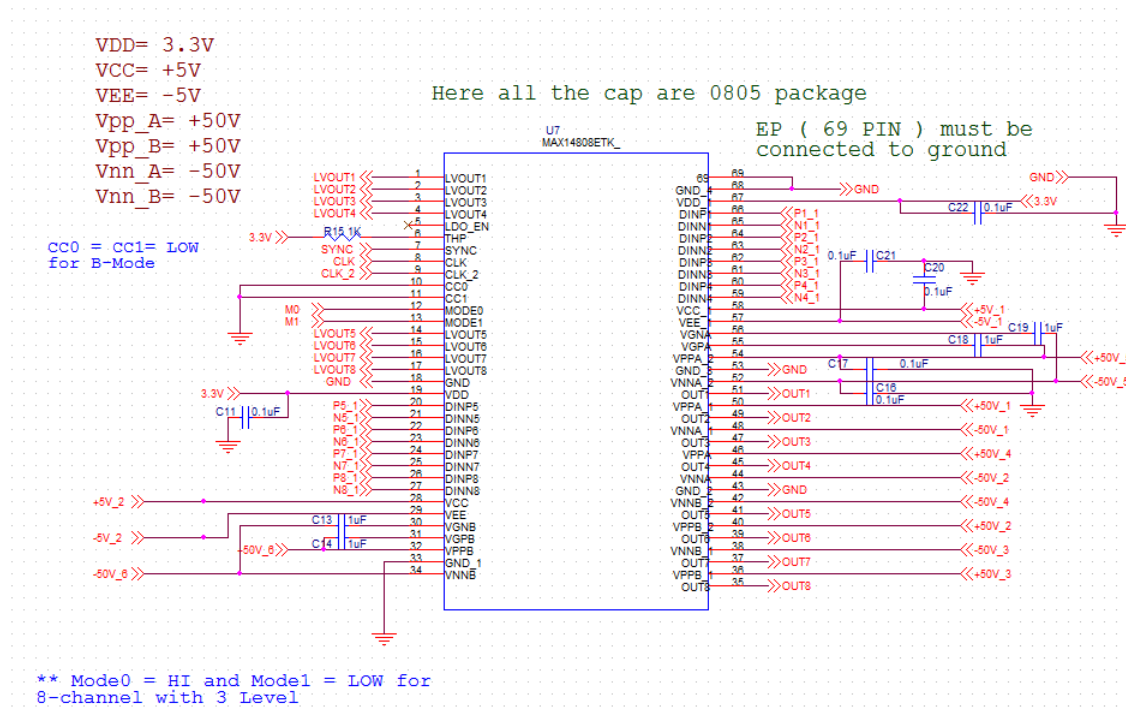


Figure 2.12: Orcad schematic for HV pulser board.

2.2.5 User interface

A Graphical User Interface (GUI) shown in Fig. 2.14 has been developed with National Instrument LabVIEW (Laboratory Virtual Instrument Engineering Workbench) 2012 in the Windows platform (Microsoft Corp., Redmond, WA). Spartan-3E starter kit is connected to a commercial PC through USB2.0 and interfaced LabVIEW project as shown in Fig. 2.15. This can provide extensive user control of transmission parameters during pulse-echo experiments. Multiple transmission parameters for each of 8 channels can be modified, including coarse time delay and fine time delay. Other parameters, such as operating frequency of ultrasound, pulse pattern length, pulse repetition rate are selected for all channels. All these parameters can be saved and loaded for B-mode imaging researches.

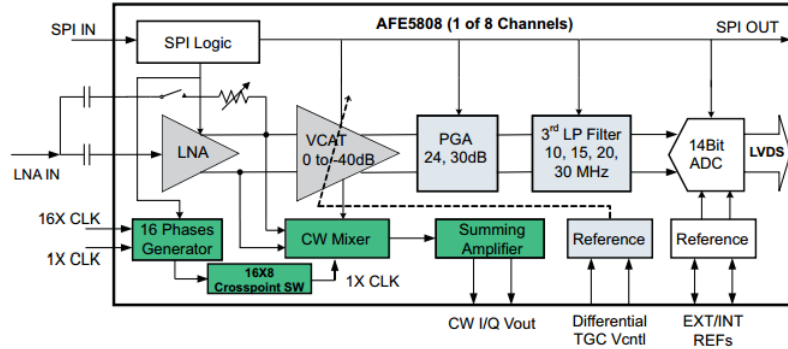


Figure 2.13: Functional block diagram of Analog Frontend.



Figure 2.14: User interface to control the transmission parameters

2.2.6 Main features of the proposed ultrasound transmit platform

- Programmable 8 independent transmit channels to drive eight transducer elements, which can be extended to more number of channels.
- High speed serial interface for 8-channel with data rate up to 80Mbps.
- Flexible user interface to select and modify transmission parameters.
- Maximum ultrasound transmit output bandwidth 80 MHz.
- Supports 4-64 bit programmable pulse pattern.
- Minimum time delay of beamformer $0.78ns$.
- The HV pulser also features 8-integrated transmit receive (T/R) switches.
- Flexibility to examine the output signals at each stage of the system.
- Our design for 8-channel transmit module is a low complex hardware and inexpensive ($\approx \$166$) compared to existing transmit modules for research purposes.

2.2.7 Comparative study with literature

Our design exploits the latest digital electronic technology to realize a low hardware complex, relatively inexpensive ultrasound transmit system. The existing transmit platforms in the literature are

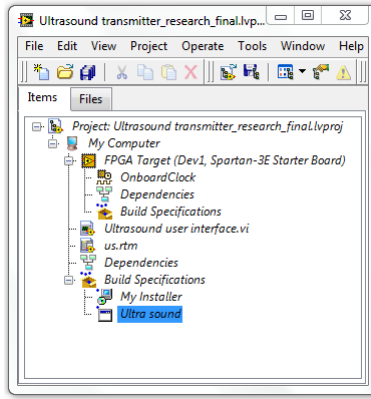


Figure 2.15: LabVIEW project interfaced to Spartan-3E FPGA Starter Kit

using additional expensive electronics for each channel [8]. The hardware of our proposed Tx architecture is optimized with the usage of high performance 8-channel Application Specific Integrated Circuits (ASICs) for Tx beamformer and HV pulser as shown in Fig. 3.1. A flexible user interface as shown in Fig. 2.14 is provided with accurate control of transmission parameters for ultrasound transmit researches.

2.3 Conclusion

In this chapter, we have presented the development of a programmable 8-channel ultrasound data acquisition for medical ultrasound research activities. Researchers can use our design to implement new receive beamforming and signal processing algorithms to optimize the image quality with extensive user control of transmission parameters. A user interface was developed to control time delays, pulse repetition frequency (PRF), pulse pattern length and operating frequency. The FPGA based ultrasound transmit platform was developed using a reasonably inexpensive FPGA starter board, two in-house made boards for Tx beamformer and HV pulser. The further optimization of transmit beamforming technique and user interface is necessary to facilitate the development and test of more transmit techniques such as Continuous Wave Doppler (CWD).

Chapter 3

Digital Ultrasound beamformer

3.1 Introduction

In commercial ultrasound systems, the multi-element transducer array is connected to analog front end electronics using long-wire high voltage coaxial cables. This chapter presents the circuit design of 16-channel Transmit (Tx) and Receive (Rx) beamforming ASIC (Application Specific Integrated Circuit) that can be integrated in ultrasound probe head which reduces the number of coaxial cables. The proposed modular design for programmable 16-channel transmit beamformer provides user control of transmit parameters such as transmit pulse length, pulse pattern, transmit frequency, and mode of excitation. The receive beamformer implements delay and coherent sum of the digitized echoes from 16 adjacent transducer elements to form scanlines required for image reconstruction. The proposed architecture of the Rx beamformer design provides great flexibility for beamforming, such as receive focusing with predetermined delay profile. Each transmit channel can be programmable to give a maximum delay of $163.85 \mu s$ with 1.25 ns delay resolution. The proposed design implements dynamic receive focusing with minimum time delay resolution of 3.125 ns for 40 MHz input data rate. The proposed ASIC of integrated Tx and Rx beamformer is implemented in UMC 130 nm technology using Synopsys ICC and Design Compiler. The implementation reports show that the area is 5.29 mm^2 , power dissipation is 38 mW .

Medical diagnostic applications using ultrasound systems are becoming prominent in diagnostic surgeries, investigating cardiovascular diseases in ambulatory and hospital divisions [6]. These applications requires handheld ultrasound scanning systems for instant diagnose of patient conditions which are battery driven and needs low power ASICs for ultrasound imaging. In ultrasound systems the digital beamformer typically generates necessary logic pulses with proper timing and phase to enable electronic steer and focus of the acoustic beam. However, these systems often have "closed" architecture that provides limited access to the researchers to perform digital ultrasound beamforming [7]. Current generation ultrasound systems are using arrays of transducer elements that are connected to front end electronics using long wire coaxial cables [16]. So, we have proposed the architecture for Tx and Rx beamforming ASIC which can be integrated in ultrasound probe head.

In the past, several digital beamformer architectures have been proposed to meet the requirements of high performance ultrasound imaging systems. In [17] authors discussed the evolution and basics

of digital beamformers. Hu et al. have presented the design and development of 16 channel digital beamformer for high frequency linear array transducers in [18]. In [16] John et al. have proposed the architecture for 8 channel transmit beamformer ASIC integrated with high voltage pulser. The existing methodologies does not provide much user reconfigurability of the transmit parameters for beamforming and limited for dynamic configuration of number of active channels.

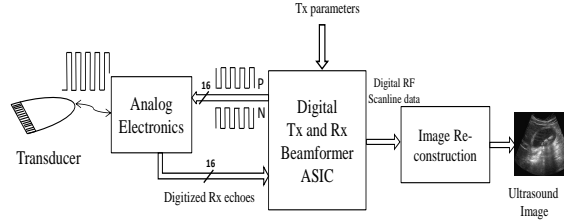


Figure 3.1: The ultrasound imaging system architecture with the proposed digital beamformer

In this chapter, we have designed the 16-channel Tx and Rx digital beamformer ASIC for ultrasound imaging which can address some of problems above discussed. The ultrasound system architecture with the proposed digital beamformer is shown in Fig. 3.1. The modular design of Tx and Rx beamforming has been developed using Verilog HDL in ISE 14.4. The modular design of Tx beamforming is provided with high speed serial interface to configure the Tx parameters such as transmit frequency, pulse length, number of active channels and mode of excitation. The proposed digital beamformer is having a provision to choose number of active channels which can be used to implement Synthetic Transmit Aperture (STA) [19] beamforming algorithm for ultrasound imaging.

For B-mode applications, the LUT (Look up Table) is configured with delay profile for Tx acoustic beam steering in the field of view which are pre-calculated using transducer parameters. The Rx beamforming architecture acquires digitized echoes of each channel that are delayed for pre-determined delay profile and coherently summed to form digital RF (Radio Frequency) scanline data. The time delays applied to real-time echo signal samples as a combination of coarse delay and fine delay. The coarse delay is integer multiples of ADC sampling period and the fine delay is a fractional time delay. The digital RF scanline data is further processed for image reconstruction to acquire ultrasound image of patient tissue. The ASIC for the proposed the design is implemented using UMC 130 nm technology using Synopsys ICC and Design Compiler.

3.2 Transmit Beamforming Architecture

The ultrasound imaging involves a typical acoustic beamsteering called as Tx beamforming which can be achieved by applying time delay of excitation to series of transducer elements [20], [21]. The modular design of transmit beamforming architecture is shown in Fig. 3.3. The Start Tx control signal is used to enable transmit and receive modes of ultrasound sensors. The design has a provision to configure different Tx parameters such as mode of transducer selection, the number of active channels, and a programmable register to choose the transmit parameters such as pulse

width adjustment, pulse pattern control, and modes of transmissions like continuous wave and pulse repetition frequency that provides an ease of user accessibility for transmit beamforming.

The time delays can be obtained using simple geometry as illustrated in Fig. 3.2 [22]. Average ultrasound velocity in tissue is considered as 1540 m/s. First, each element is treated as a point source located at the geometric center of the physical element. As the delays used in transmit beamforming are additive delays, the difference between these distances and the distance from the outermost element is then calculated. This gives the difference in travel distance for the acoustic waves that must be corrected for using electronic delays. 3.2 explains the time-delay value calculation for each element [22]. Fig. 3.3 shows the modular architecture for the transmit beamforming to steer and focus the acoustic beam.

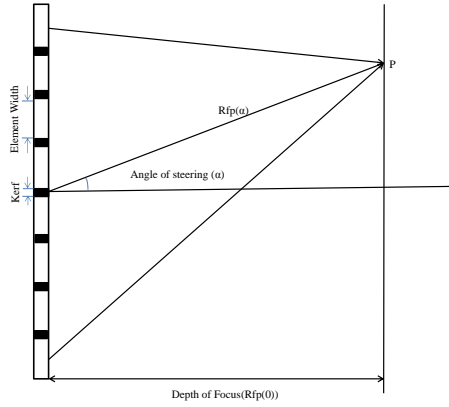


Figure 3.2: Calculations of delay profile for a steering angle (α°)

$$t_i = \frac{\sqrt{R_{fp}^2(\alpha) + x_i^2 - 2x_i R_{fp}(\alpha) \sin(\alpha)}}{c} \quad (3.1)$$

$$\text{where } R_{fp}(\alpha) = \frac{R_{fp}(0)}{\cos(\alpha)}$$

$$T_i = t_{max} - t_i \quad (3.2)$$

$P \rightarrow$ Focal point.

$R_{fp}(\alpha), R_{fp}(0) \rightarrow$ Distance from center element to point P

$t_i \rightarrow$ Time required for wave front to reach point P.

$x_i \rightarrow$ Co-ordinate of i^{th} element.

$t_{max} \rightarrow$ Max time required for wave front to reach point P.

$T_i \rightarrow$ Delay for i^{th} element.

The proper time delays for beam steering are obtained from equation (3.1) and (3.2). These delay

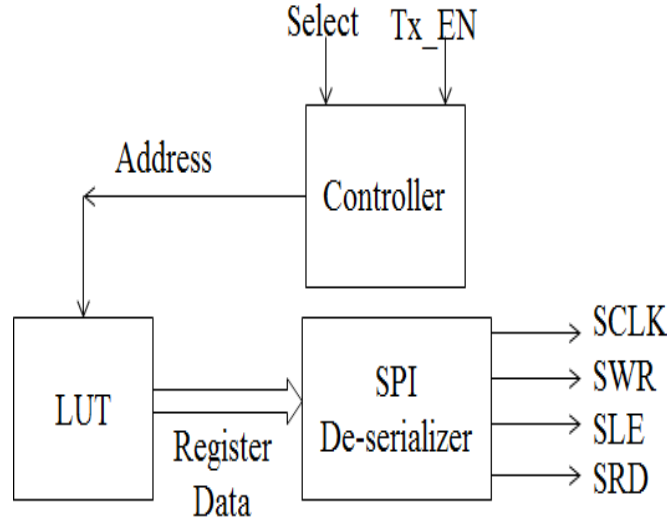


Figure 3.3: Modular architecture for proposed Transmit beamforming

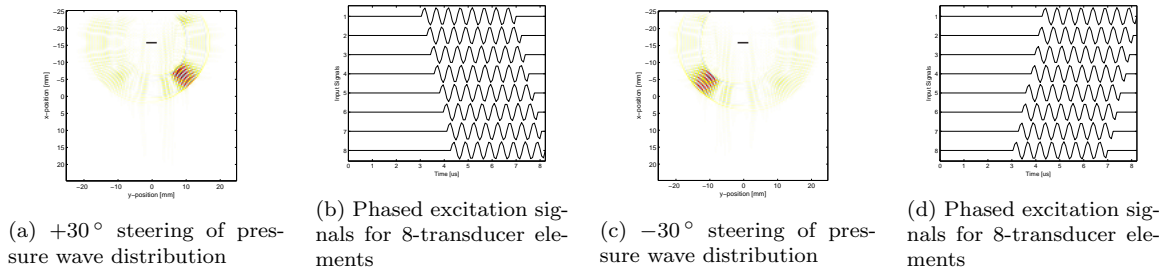


Figure 3.4: Simulation results

profile per scanline at a given steering angle are simulated using software tool. Fig. 3.4 shows pressure wave distribution in 2-D and phase delays of burst signal for each transducer element for $+30^\circ$, -30° respectively.

3.3 Receive Beamforming Architecture

The digital receive beamforming is essential for attaining good image quality by increasing signal-to-noise ratio (SNR), improving spatial resolution and reducing sidelobe artifacts [23]. The received echoes of each transducer elements are connected to ADC (Analog to Digital Converter) after signal conditioning further the digitized echo signal is time delayed by predetermined delay profile and coherently summed to form RF scanline data. The RF scanline data is then processed for image reconstruction to acquire ultrasound image. Fig. 3.2 shows the simple geometry of transducer elements and field of view to the focal point. The delay profile for each transmission to perform dynamic receive focus is obtained from equations (3.1), (3.2) for transducer physical parameters which are stored as LUT in the design. Average ultrasound velocity (c) in tissue is considered as 1540 m/s.

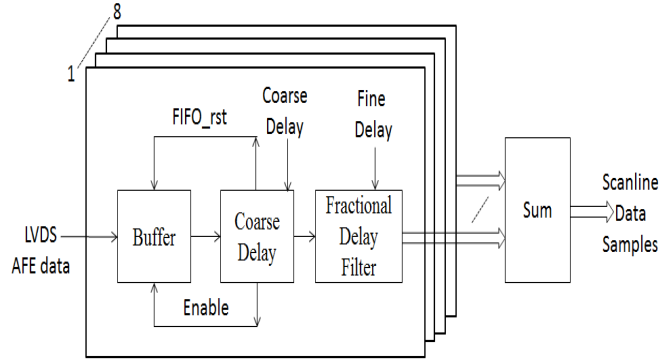


Figure 3.5: Modular architecture for proposed receive beamforming.

Fig. 3.5 illustrates the proposed modular architecture for receive beamforming. The design buffers real-time digitized echo samples per each channel from analog electronics at a rate of ADC sampling frequency (40 MHz). The delays are applied to the real-time echo samples in terms of coarse delay and fine delay. The coarse delays are integer multiples of the clock periods and the fine delays are applied with an interpolation filter [24]. The dynamic receive focusing is implemented based on state machine which updates delay values and the interpolation filter coefficients according to the steering angle of acoustic beam. The scanline data which is fed to image reconstruction can be obtained by coherent sum of delayed echo samples of each channel.

The modular design buffers the echo signal samples in receiving mode, which is controlled by Start Tx control signal. The coarse delay applied in terms of integer multiples of ADC sampling period ($0.25 \mu s$) and an interpolation filter is implemented by a factor of 8, which enables a minimum fractional delay of $(1/8)^{th}$ of the ADC sampling period (3.125 ns). Fig. 3.6 shows the simulation result of Rx beamforming design for four individual channels. The input data samples are fed at a rate of 40 MHz which is latched for every rising edge of the clock. The input data is delayed by number of samples according to respective delays and summed to form RF scanline data samples.

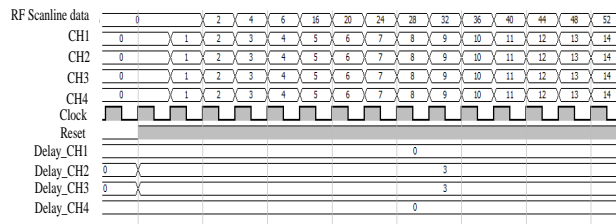


Figure 3.6: Simulation result of Rx beamforming design.

3.4 ASIC Implementation

Area, power dissipation and speed are the most important factors when it comes to implementation of high end systems in VLSI domain [25]. The integrated design of 16-channel Tx and Rx beamformer has been simulated using Synopsys VCS (Verilog Compiler Simulator), synthesized using DC (Design Compiler) and implemented the complete physical design using ICC (Integrated Circuit Compiler). Fig. 3.7 shows the Gate level simulation (GLS) obtained for the proposed architecture. Here the two individual channel logic outputs of Tx beamformer are simulated according to the delay profile programmed in delay registers. The ASIC implementation of the design is carried out in UMC 130 nm 3.3/1.2V 8 metal layer CMOS process technology and fabricated as DIL-16 (Dual in-line package). An area of about 5.29 mm^2 , 292 K equivalent gates dissipates 38 mW (from 1.2V) while operating at 20 MHz. TABLE 3.1 shows the chip characteristics of the proposed design. Fig. 3.8 is the final layout of the integrated 16-channel Tx and Rx beamformer.

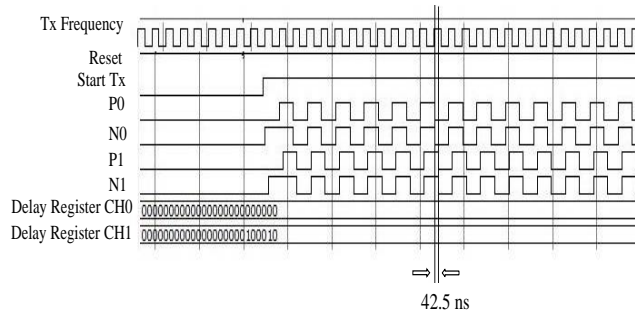


Figure 3.7: Gate level simulation results in Design Compiler.

Table 3.1: Chip characteristics

Technology	UMC 130 nm 3.3/1.2V
Area of chip	5.29 mm^2
Reference Frequency	20 MHz
Power dissipation	38 mW
Number of logic gates	292K
Package	DIL 16

3.5 Conclusion

We have designed the integrated 16-channel Tx and Rx beamforming ASIC for portable ultrasound imaging. From the results we can infer that the design achieves a relative timing difference between

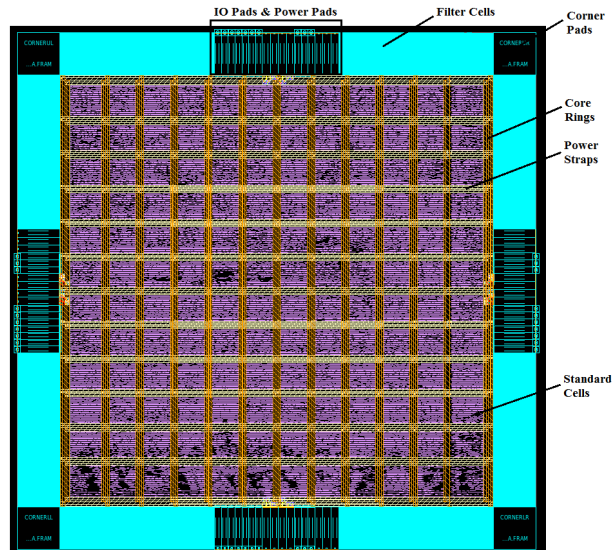


Figure 3.8: Layout of ASIC of proposed architecture for integrated Tx and Rx beamformer.

two individual channels with a minimum delay resolution of 0.78 ns and maximum of 102.6 μs for Tx beamforming. While the dynamic receive focusing with the smallest time delay resolution of 3.125 ns for the 40 MHz echo signal samples. The fabricated chip for the proposed design with area 5.29 mm^2 , 292 K equivalent logic gates dissipates 38 mW (from 1.2V) while operating at 20 MHz which accomplishes the design suitable for portable ultrasound imaging systems.

Chapter 4

Validation and Evaluation of the prototype

4.1 Introduction

We have integrated ultrasound signal processing modules such as Data Acquisition System and image reconstruction modules to form a portable ultrasound imaging system. We have also integrated an embedded processor to the ultrasound system. The embedded processor is provided with security authentication and GPS module. This additional technical interfaces facilitates the device for secure we based diagnosis. The prototype for secure portable ultrasound imaging system is meets the current generation requirements in POC applications. The portable device can be operated for real time imaging of tissue organ thus offers quick diagnosis in remote locations such as battle fields and Ambulances.

Our Ultrasound Data Acquisition System is validated by scanning a customized phantom. We also evaluated the some frontend specifications of the system such as spatial resolution and time required to acquire one frame.

4.2 Prototype of secured, IoT enabled portable ultrasound system

Fig. 4.1 shows a prototype of our secured, IoT enabled portable ultrasound imaging system developed. The prototype is designed for 32-channels. The system specifications and interfaces to the portable ultrasound system developed are summarized in Table 4.1. Our prototype for portable ultrasound system can support the B-mode imaging. As shown in Fig. 4.2, the main board consists of Application Specific Integrated Circuits(ASICs) for logic pulse driver, HV pulser, analog receiver each of four in number and Zynq 7000 SoC. The power supplies of the whole boards are $\pm 5V$ and HV pulser driving supplies are $\pm 50V$ and safe connectors are provided to power up the board.

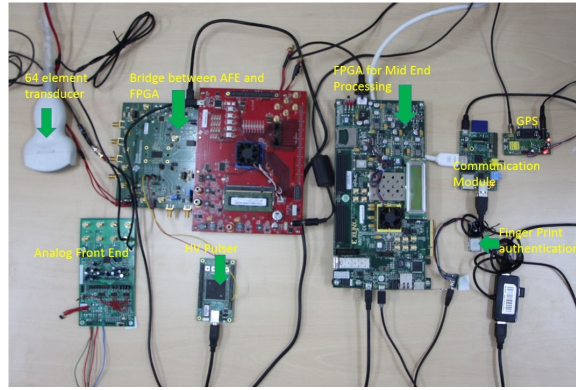


Figure 4.1: Prototype of secure and IoT enabled portable ultrasound systems

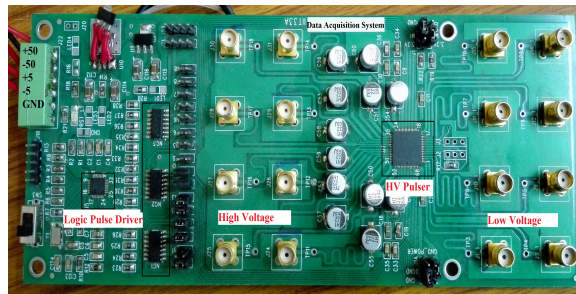


Figure 4.2: Portable ultrasound scanner module.

4.2.1 Phantom Experiment with Our Portable Ultrasound Imaging System

The parameters of the transducer and hardware setup used in the phantom experiment are summarized in Table 4.2. The beamforming was performed for each transmission to form sharp ultrasound beam while in reception to obtain scanline data. For the phantom experiment, a customized tissue-mimicking phantom is designed in our laboratories. It was scanned with a 7.5-MHz linear array transducer.

Fig. 4.3 shows the captured image using a 7.5-MHz linear array transducer with the developed prototype portable ultrasound system from tissue-mimicking phantoms with imaging depths of 5 cm. As shown in Fig. 4.3, the portable system developed can clearly show the curvature of the reflecting target up to 5 cm.

4.3 Validation With other Platforms

4.3.1 PXI System

Commercially there are some platforms for instrumentation, measurement and control. National Instrument's PXIe-1078 Platform for Test, Measurement, and Control. PXI combines PCI express features with the modular, Eurocard packaging of CompactPCI and then adds specialized synchronization buses and key software features. PXI is having 16 high speed analog input channels to

Table 4.1: System specification of our secured, IoT enabled portable ultrasound imaging system

Number of channels	32
ADC sampling frequency	40 MHz
Processing System (PS)	Raspberry PI
Operating System (OS)	Linux
Programmable Logic (PL)	Kintex 7
Peripherals	SD Card, 2 USB OTG ports, 1 USB UART port, LAN, VGA, and HDMI ports for external monitor
3G data rate	2 - 28 Mbit/s
Finger print scanner	GT-511C3
GPS device	RoyalTek RE 1315S4

Table 4.2: Parameters of phantom experiment setup.

Specification	value
Transmit frequency	5MHz
Number of channels	32
Kerf of transducer	.025 mm
Element width	.154 mm
Depth of scan	50 mm
Field of view	-60° to $+60^\circ$
Number of scanlines	192

acquire sensor data and digitization. We have interfaced our data acquisition board to the PXI analog channels. Here a spartan 3 FPGA is used to establish synchronisation between PXI and our module. Fig. 4.4 shows the hardware for PXI platform setup. Our ultrasound board is provided with some control pins to programme the transmission parameters for logic pulse driver. The FPGA generates a transmit control signal which is used as synchronisation of PXI and ultrasound front end board. The PXI system uses LABVIEW 2013 software to acquire high speed ultrasound data and reconstruct ultrasound image. We have used a linear array transducer with centre frequency of 7.5 MHz to scan our customized phantom. Fig. 4.5 is the reconstructed image where our data acquisition system is used to acquire ultrasound sensor data and formed the image in PXI system. The reconstructed image is shows that our data acquisition module able to acquire the ultrasound data.

4.3.2 Biosono Frontend Platform

Our Ultrasound DAQ is also compared with Biosono frontend platform. Fig. 4.6a shows the Biosono board with single element probe of A-mode and M-mode imaging applications. SonoLab series products provide convenient solutions for non-human use ultrasound application such as education, ultrasound related research, and prototype development. The whole system is on a single PCB board powered by a DC supply, which can be as simple as a commonly used DC adapter with voltage around 7v to 15v, and a current rating above 1A. It transmits square wave burst with predefined peak-to-peak voltage up to 200V and programmable pulse length and pulse repeat frequency (PRF).

The echo is sampled and digitized at rate of 100MHz, and streamed out at the serial port at 115200 bps. A free Matlab GUI (Fig. 4.6b) is provided to view the real time echo. The multiply

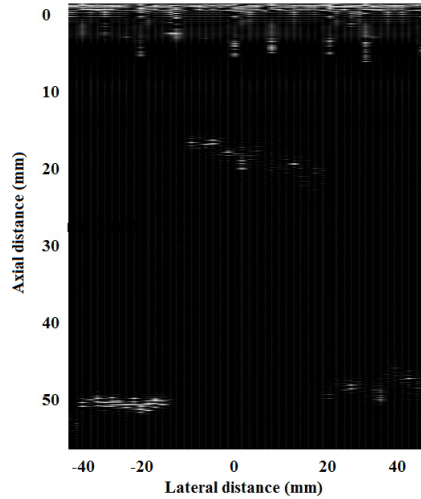


Figure 4.3: Acquired ultrasound image from phantom.

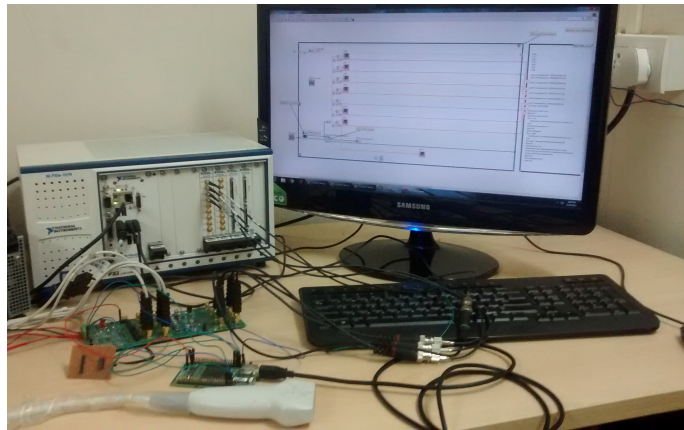


Figure 4.4: Validation with PXI platform.

of transmitting pulse amplitude, pulse length, and PRF is a constant when the load is fixed. So, if you increase one parameter, the maximal allowed value for other two parameters will be lowered automatically. We have used the single element transducer to scan our customized phantom to acquire ultrasound and the reconstructed ultrasound image shown in Fig. 4.7.

4.4 Calculations for B-Mode Imaging

The spatial resolution of a B-mode image can be evaluated into lateral resolution and axial resolution. It represents the smallest distance, the reflectors can be separated and still be distinguishable as separate points [26]. Higher frequencies are in principle more desirable, since they provide higher resolution but limited by tissue attenuation [27]. Short ultrasound pulses are required for better lateral resolution of image [28]. Fig. 4.8a, Fig. 4.8b illustrates the definitions of axial and lateral resolutions respectively.

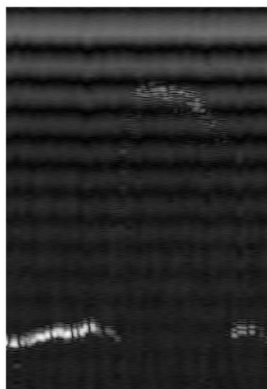
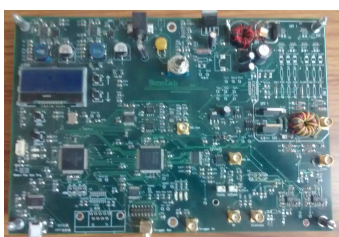
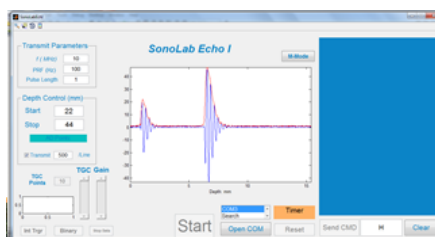


Figure 4.5: Acquired ultrasound image with PXI setup.



(a) Biosono frontend board.



(b) GUI for Biosono board

Figure 4.6: Biosono Platform.

The axial resolution is determined by the length of the ultrasound pulse. It is limited by the spatial pulse length (SPL). Reflectors closer to one another than half the SPL cannot be resolved. The shorter the SPL, better the axial resolution. Typically, the SPL is of the order of 1-3 wavelengths of the beam. Since frequency and wavelength are inversely related, the SPL will decrease with increasing beam frequency. Therefore, the higher the beam frequency, the better the axial resolution.

$$Axial\ resolution = \frac{SPL}{2} = \frac{n * \lambda}{2}$$

In ultrasound imaging, axial resolution is better than lateral resolution, besides showing less variation. The lateral resolution of a beam is dependent on the focal depth, the wavelength and probe diameter (aperture) of the ultrasound probe. The factors affecting lateral resolution be well understood. These factors include:

- Beam Width
- Beam frequency
- Scanline density

$$Lateral\ Resolution = \frac{d * \lambda}{D} = 5.45mm$$

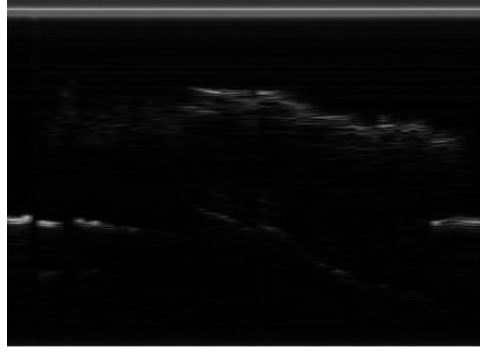
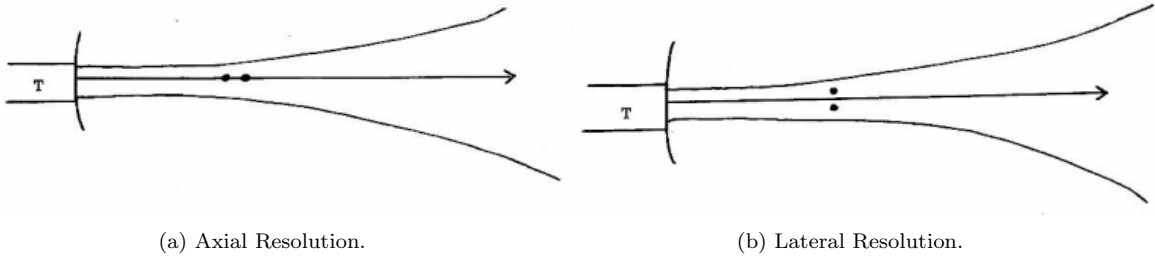


Figure 4.7: Acquired ultrasound image using Biosono frontend board.



(a) Axial Resolution.

(b) Lateral Resolution.

Figure 4.8: Spatial Resolution of ultrasound image.

The time required to acquire one frame is depends on the number of scanlines for frame and depth of scan. Given the depth of scan, higher the frame rate, lower will be the scanline density in region of interest.

$$\text{frame rate} = \left(\frac{2*d}{c}\right) \left(\frac{\theta}{\Delta\theta}\right) = 16.384msec$$

where

n → Number pulses in transmit beam

d → depth of scan.

c → Average velocity of ultrasound (1540 m/s)

λ → Beam wavelength

θ → Field of view

$\Delta\theta$ → Angular Resolution

Chapter 5

Conclusions

5.1 Review of Thesis Work

This thesis has presented the work done designing, building, and testing a versatile ultrasound data acquisition system. We Proposed a design based on the Delay and Sum digital beamforming implementation, it is consists of a 8 channel frontend signal processing board. The modular nature of the design allows the hardware to expand to the size needed by any front-end transducer, from the largest 2D arrays, to the smallest annular devices. For all of these advantages, the hardware is small, efficiently designed, and leverage the best of consumer electronics in order to minimize the actual system cost. The total expected cost per channel is between 25and40 The HDL firmware that has been created for the signal processing card is extremely optimized using Xilinx ISE at processing ultrasound data. The Firmware to be extended to perform additional real-time signal processing taken as a whole, the beamformer system is fast, robust, versatile, cost-effective, and easy to use. All tests performed on individual component of it, have shown that desired performance has been met. This design will provide an ideal open programmable platform for researchers. We have conducted with the prototype to scan the customized phantom and acquired an Ultrasound image with axial resolution of 0.616mm while the lateral resolution of 5.45mm.

5.2 Conclusions

This thesis has looked into a proposed low cost implementation of the digital beamformer based on the FPGA. We described a novel extendable Beamforming architecture design in the both of the system-level Hardware and Firmware design level. In the Hardware design, we were targeting the compactable application as well as the extendable applications where the power, level of integration and the feasible of the replication are critical. The three main components that have the greatest influence on the hardware design and system performance of the signal-processing board are the Analog to Digital Converters (ADCs), the Beamformer transmitter and the FPGA. Moreover we described gradual shift of beamforming from analog to digital and also traced the evolution of digital beamformers to its present day commercial implementations. With digital beamforming, the advantage of it over conventional analog beamformers has been brought out by comparing its performance with the simulated analog beamformer implementation. Digital beamforming does help

in improving the image quality and has improved lateral resolution compared to analog beamformers. Also the increased dynamic range in a digital beamformer is due to the dynamic receive focusing. Our proposed design based on the Delay and Sum. The Delay and Sum architecture produces high resolution images but at a high cost due to the many parallel transmits and receives channels. This method produced images with poorer lateral resolution and was susceptible to motion artifacts, but helped in increasing the frame rate that is suitable to do 3-D imaging. Also the system complexity is lower due to the low channel count.

References

- [1] M. C. Z. H. D. R. F. A. D. S. B. Barnett, G. R. Ter Haar and K. Maeda. International recommendations and guidelines for the safe use of diagnostic ultrasound in medicine Vol. 26, (March 2000) pp. 355–366.
- [2] L. Bassi, E. Boni, A. Cellai, A. Dallai, F. Guidi, S. Ricci, and P. Tortoli. A Novel Digital Ultrasound System for Experimental Research Activities 413–417.
- [3] Y. M. Yoo, F. Schneider, A. Agarwal, T. Fukuoka, K. L. Mong, and Y. Kim. Ultrasound Machine for Distributed Diagnosis and Home Use 63–66.
- [4] K. Abd-Elmoniem, A.-B. Youssef, and Y. Kadah. Real-time speckle reduction and coherence enhancement in ultrasound imaging via nonlinear anisotropic diffusion. *Biomedical Engineering, IEEE Transactions on* 49, (2002) 997–1014.
- [5] U. D. M Ali, D Magee. *Texas Instruments* .
- [6] A. Chiang, P. Chang, and S. Broadstone. PC-based ultrasound imaging system in a probe 2, (2000) 1255–1260 vol.2.
- [7] L. Bassi, E. Boni, A. Cellai, A. Dallai, F. Guidi, S. Ricci, and P. Tortoli. A Novel Digital Ultrasound System for Experimental Research Activities 413–417.
- [8] A. Assef, J. Maia, F. Schneider, E. Costa, and V. da Silveira Nantes Button. A programmable FPGA-based 8-channel arbitrary waveform generator for medical ultrasound research activities 515–518.
- [9] J. Alexander. Xilinx Devices in Portable Ultrasound Systems. Technical Report, Xilinx, Inc. May 13, 2013.
- [10] G. Cincotti, G. Cardone, P. Gori, and M. Pappalardo. Efficient transmit beamforming in pulse-echo ultrasonic imaging. *Ultrasonics, Ferroelectrics, and Frequency Control, IEEE Transactions on* 46, (1999) 1450–1458.
- [11] V. Chan and A. Perlas. Basics of Ultrasound Imaging .
- [12] S. S. M. R. S. S. R. K. Saha, S. Karmakar and S. Sen. Ultrasonic Linear Array Medical Imaging System .
- [13] T. Instruments. LM96570 Ultrasound Configurable Transmit Beamformer. Technical Report September 15, 2011.

- [14] I. Maxim Integrated Products. MAX14808/MAX14809 Octal Three-Level/Quad Five-Level High-Voltage 2A Digital Pulsers with T/R Switch. Technical Report March 2013.
- [15] T. Instruments. AFE 5809 Fully Integrated, 8-Channel Ultrasound Analog Front End. Technical Report SLOS738D SEPTEMBER 2012.
- [16] K. S. C. John V. Hatfield. A beam-forming transmit ASIC for driving ultrasonic arrays .
- [17] K. Thomenius. Evolution of ultrasound beamformers 2, (1996) 1615–1622 vol.2.
- [18] C. Hu, X. chen Xu, J. Cannata, J. Yen, and K. Shung. Development of a real-time, high-frequency ultrasound digital beamformer for high-frequency linear array transducers. *Ultrasonics, Ferroelectrics, and Frequency Control, IEEE Transactions on* 53, (2006) 317–323.
- [19] G. Lockwood, J. Talman, and S. Brunke. Real-time 3-D ultrasound imaging using sparse synthetic aperture beamforming. *Ultrasonics, Ferroelectrics, and Frequency Control, IEEE Transactions on* 45, (1998) 980–988.
- [20] G. Cincotti, G. Cardone, P. Gori, and M. Pappalardo. Efficient transmit beamforming in pulse-echo ultrasonic imaging. *Ultrasonics, Ferroelectrics, and Frequency Control, IEEE Transactions on* 46, (1999) 1450–1458.
- [21] C. R. C. John A. Hossack, Jian-Hua Mo. Transmit beamformer with frequency dependent focus. *U.S. Patent 5696737 A* .
- [22] T. Instruments. Signal Processing Overview of Ultrasound Systems for Medical Imaging. Technical Report SPRAB12 November 2008.
- [23] C. R. C. John A. Hossack, Jian-Hua Mo. Software-based ultrasound phase rotation beamforming on multi-core DSP. *Ultrasonics Symposium (IUS), 2011 IEEE International* .
- [24] C. Hu, K. Snook, X. chen Xu, J. Yen, K. Shung, and P. jie Cao. FPGA based digital high frequency beamformers for arrays [ultrasonic eye imaging applications] 2, (2004) 1347–1350 Vol.2.
- [25] P. Kannan, A. Pulli, and K. Govindarajan. A VLSI - ASIC implementation of Fast Hartley transform for OFDM receivers 609–613.
- [26] D. Kouame and M. Ploquin. Super-resolution in medical imaging : An illustrative approach through ultrasound 249–252.
- [27] E. Brunner. How Ultrasound System Considerations Influence Front-End Component Choice. Technical Report, Analog Devices, Inc. 2002 Volume 36, Number 3, May-July, 2002.
- [28] J. S. M. C. F. F. M. Alexander Ng MB ChB FRCA MD. Resolution in ultrasound imaging .